Egyptian Journal of Chemistry

http://ejchem.journals.ekb.eg/

Enhancement Adsorption of Crystal Violet From Wastewater Using Chemically Modified Sugarcane Bagasse by Bentonite and Polyurethane

Sabah S. Ibrahim [a], Mohamed M. El Bouraie [a], Yasmeen R. Abdallah [b]*, Yasser K. Abdel-Monem [b]

[a] *Central Laboratory for Environmental Quality Monitoring, National Water Research Center, El-Kanater, Egypt.*

[b] *Menoufia University ,Faculty of Science, Chemistry Department, Shebien ElKoom, Menoufia , Egypt.*

Abstract

The suitability of the sorbent material derived from bagasse (chemically modified with bentonite and polyurethane for adsorption of crystal violet from an aqueous solution was evaluated in a series of batch adsorption experiments). A batch adsorption study was investigated to study the effect of pH, initial dye concentration, adsorption doses, and contact time at different temperatures. The best fit for the adsorption kinetics data is a pseudo-second-order model, while the best description for the adsorption equilibrium data is the Langmuir isotherm. Thermodynamic studies of the adsorption process were performed, and the variables, entropy (ΔS^o), enthalpy (ΔH^o), free energy (ΔG^o), were determined. The endothermic character of the adsorption process was demonstrated by a rising trend in adsorption with increasing temperature.

Key Words: Chemically modified; Bentonite; Crystal Violet; Adsorption; Thermodynamic Parameters

1. Introduction

At present, with the advancement of the global economy of the industry, organic dyes are often used to color various industrial materials such as textiles, leather tanning, plastics, cosmetics, paper, and paint, which led to contamination of a huge amount of sewage with various pollutants, including toxic compounds, dissolved solids, acids, and bases. They are aesthetically uncomfortable and also hinder light penetration into plants, and then affect the photosynthesis process of aquatic organisms. Furthermore, many dyes are poisonous to some bacteria, causing direct harm to their catalytic capability or stabilising it. There are more than 1 x 10^5 commercial dyes with an estimated production of 7 x 10^5 – 1 x 10^6 tons per year of this mass production [1]. No exact data is available on the number of dyes that are discharged into the environment. However, it has been reported that 10-15% of used dyes enter the environment from waste [2, 3]. Among these effluents, crystal violet (CV) dye is widely used as a protein-dye that is used for fingerprint identification and is also used in most types of adhesive taps for later printing. They are also used in Gram stain for all demonstration and basic classification of dyes brilliant colors are produced using CV which belongs to the triphenyl methane group. They are widely used in veterinary medicine It is the brightest class of basic dyes with high micro value [4]. They enter the human body through inhalation, ingestion, and skin absorption. They can lead to severe health damages to humans such as arrhythmias, vomiting, tissue necrosis, kidney cirrhosis, skin allergy, cancer, impaired function of the brain and central nervous system. Hence, elimination of untreated effluent to the surrounding environment often creates problems for aquatic life and humans. To avoid any potential risks, there is a need for effective treatment of this industrial wastewater before it is discharged into the environment. Various treatment methods for decolorization and dye removal are ion exchange,

*Corresponding author e-mail: redayasmeen581@gmail.com; (Yasmeen R. Abdallah)

Receive Date: 07 March 2022, **Revise Date:** 09 May 2022, **Accept Date:** 11 May 2022, **First Publish Date:** 11 May 2022
DOI: 10.21608/EJCHEM.2022.125800.5590

coagulation, membrane separation processes, photolysis, biological treatment, chemical oxidation, and adsorption and they have been widely applied in the process of removing dyes from aqueous solution [5-13]. Because of its ease of use, high efficacy, and wide range of inexpensive sorbents, adsorption is a promising strategy for eliminating dyes among the many treatment methods. Clays, porous materials, activated carbon, zeolite, natural or agro-industrial by-products, and other adsorbents have all been produced in this regard to separate and remove various dyes [14]. Although sorbents are considered promising materials for removing pollutants, raw sorbents (without modification) suffer from their low sorption efficiency. Therefore, in this study, sugarcane bagasse (SCB) was chemically modified by a composite of bentonite and polyurethane and chemically activated using the chemical agent H_3po_4, for enhancing the absorption capacity of biomass by increasing the specific surface area and introducing various chemical functional groups [14]. Considering the above reasons in this study, we chose it, as a new and promising adsorbent for removing cationic dyes from aqueous solutions. Various parameters such as pH, adsorbent dosages, initial dye concentration, contact time, and temperatures were investigated. The batch adsorption study used kinetic and equilibrium data to better understand the adsorption process.

2. Materials and Methods

2.1. Dye Solution

CV, λ = 583 nm, molecular formula $C_{25}H_{30}ClN_3$, also known as Tris(4-(dimethyl amino) phenyl) methylium chloride, Molecular weight (g mol^{-1}) 407.99, **Fig. 1**, was purchased from Sigma–Aldrich Chemicals. By dissolving 1.0 g/L dye in deionized water, a 1000 mg/L CV stock solution can be obtained. 0.1M HCl or 0.1M NaOH was used to adjust the pH of the dye solution. At the start of each experiment, new dilutions to the required dye concentrations were prepared.

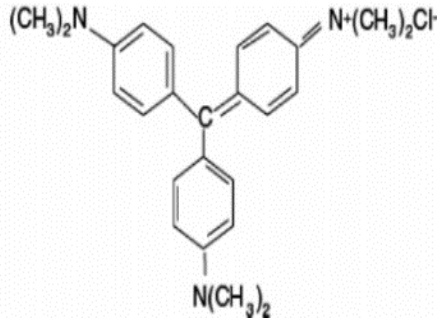

Fig. 1. Structure of crystal violet

2.2. Preparation of (SCBBPU) adsorbent

Sugarcane bagasse (SCB) was collected from a local market in Shabin Al-Qanatir, Egypt. Before use, SCB was washed gently with water to remove impurities present on the surface and then dried in an oven at 105°C all night or until constant weight to reduce moisture content. The sample was weighed to determine the dry weight and then crushed well. SCB is chemically modified by a composite of bentonite and polyurethane. SCBBPU prepared by adding a ratio of 2 sugarcane bagasse: 1 bentonite: 1polyurethane. The mixture was then agitated until the mixed adsorbent was thoroughly combined. After mixing, the mixture is baked in a 200°C oven for 30 minutes, or until it is completely charred. 50 g of SCBBPU was impregnated with 200 ml of 40% w/v H_3PO_4 solution and soaked for 24 h under anaerobic conditions; then the mixture was stirred at 85°C for 1 h to the interior of the precursor. The material was carbonized under closed conditions after impregnation. The temperature was raised to 500°C at a rate of 4°C/min for 3 hours. The mixture was allowed to cool before being rinsed to eliminate any remaining reagent. The sample was then subjected to heat at 120°C for 3 h to vaporize the water. The dried mixture was subjected to heat at a temperature of 650°C in muffle furnace to enable activation of the pores of the carbon sample. Dried biomass SCBBPU was preserved in air-tight glass bottles to protect it from moisture.

2.3. Characterization of SCBBPU

Fourier Transform Infrared spectroscopy (FT-IR) was used to determine functional groups in the sample using a (Thermo Scientific Nicolet iS10 spectrometer) in the wavenumber range of 4000–400 cm^{-1}. X-ray diffraction (XRD) was utilised to evaluate the crystalline structure of solid materials (Bruker, D8 Discovery EVA, Germany). XRD patterns were acquired at 40 kV and 40 mA, and monochromatic high-intensity Cu Kα1 (λ =1.5406 Å) was employed as the source of radiation in the spectrum (2θ) range 0° to 70°. At EDRC, DRC, Cairo, the surface morphologies of activated carbon materials were recorded using a Quanta FEG 250 Scanning Electron Microscope (SEM) (FEI Company, Hillsboro, Oregon-USA). The specific surface area and porosity were determined using the BET method on a N2 adsorption-desorption system at 77 K. (Quantachrome Corporation, NOVA I04IP001EN-A). The Henry equation was used to compute the zeta potential of the sample (Zetasizer Nano ZS fitted with an autotitrator – Malvern Instruments Ltd., UK). Absorbance of dyes was

analyzed spectrophotometrically at a wavelength of 583 nm by (UV-Vis Spectrophotometer, Evaluation 300, Evon106002) and all adsorption experiments were carried out on a magnetic stirrer at 200 rpm.

2.4. Batch adsorption experiments

The rate and equilibrium data for adsorption studies were obtained using the batch technique. Influence of value of pH, contact time, initial concentration and adsorbent dosage at different temperatures. At the chosen temperature and pH value, 100 ml conical flasks containing 50 ml of CV solution of suitable concentration mixed with 0.01–0.05 g SCBBPU were stirred at 200 rpm for different adsorption periods. A pH meter was used to monitor the initial pH of the solution, which was controlled using 0.1M NaOH and 0.1M HCl solutions. The contact duration ranged from 0 to 100 minutes, the pH was 3–9, and the temperature was 25° to 55°C, with 200 rmp stirring until equilibrium was attained. After the required time, the conical flask was removed and the adsorbent was isolated by filtration through a 45 μm Whatman filter paper. To measure the solution's remaining dye content, the supernatant was collected and examined spectrophotometrically at a wavelength of 583 nm. The findings of this research were utilized to determine the best conditions for removing dye from aqueous solutions. The amount of dye adsorbed onto activated carbons, q_e (mg/g), was determined using the equation below. (1)

$$q_e = (C_0 - C_e)v/m \quad (1)$$

The removal efficiency of dye was also calculated by using Eq. (2)

$$\%\, Removal = (C_0 - C_e)/C_0 \times 100 \quad (2)$$

Where C_o and C_e represent the starting and final amounts of dye (mg/L), V represents the volume of the solution (L), and M represents the mass of the adsorbent (g). R percent is the removal effectiveness of dye adsorbed, where q_e is the adsorption capacity (mg/g).

2.5. Kinetics model

To fit the kinetic experimental data, pseudo-first-order and pseudo-second-order kinetic models were used to investigate the adsorption mechanism. The pseudo-first-order equation may represent the beginning stages of the adsorption process, but the data may depart from the fitting curve as the adsorption process progresses. The equation below indicates the linear form of the pseudo-first-order kinetic rate equation (3) [16].

$$\log (q_{e-}q_t) = \log (q_e) - k_1 t/2.303 \quad (3)$$

The equilibrium adsorption capacity is q_e (mg/g), the amount of dye adsorbed at time t (min) is q_t (mg/g), and the rate constant of the pseudo-first-order equation is k_1 (1/min). A plot of log(q_e-q_t) vs. t revealed the adsorption rate constant, k_1, for first-order kinetics.

Chemical absorption as a rate-control mechanism is consistent with the pseudo-second-order equation. This equation is the linear form of the pseudo-second-order kinetic rate equation (4) [17].

$$t/q_t = 1/k_2 q_e^2 - t/q_e \quad (4)$$

Where q_e (mg/g) is the equilibrium adsorption capacity, q_t (mg/g) is the amount of dye adsorbed at time t (min), k_2 (g/(mg. min)) is the constant rate of the pseudo-second-order equation. The second-order rate constant k_2, and the equilibrium adsorption capacity (q_e), can be determined experimentally from the intercept and the slope of plot t/q_t vs. t, respectively.

2.6. Isotherm modeling

Adsorption equilibrium is defined as the equilibrium distribution of a given component between adsorbate and adsorbent. Isotherms equations such as Langmuir, Freundlich, and Temkin were examined to describe the equilibrium adsorption.

The Langmuir isotherm, which is derived from simple mass-action kinetics, assumes that molecules are adsorbed as a saturated monolayer of solute molecules on the adsorbent surface, with no transmigration in the plane of the surface and negligible contact between adsorbed molecules. Eq. (5) represents the Langmuir isotherm model in its linear form [18]:

$$C_e/q_e = 1/q_0 K_L - C_e/q_0 \quad (5)$$

Where C_e (mg L^{-1})symbolizes the equilibrium dye concentration in the solution, q_e (mg g^{-1}) symbolizes the amount of dye adsorbed per unit mass of adsorbent, q_0 (mg g^{-1}) symbolizes the Langmuir constant relating to the maximum monolaye^{-1}r adsorption capacity, and K_L (Lmg^{-1}) denotes the Langmuir constant relating to the free energy or net enthalpy of a The slope and intercept of the linear plot indicate that adsorption obeys the Langmuir model, and the constants q_0 and K_L are determined from the slope and intercept, respectively. The Langmuir isotherm model's fundamental properties can be described in terms of R_L, a dimensionless constant, separation factor, or equilibrium parameter that can be derived using Eq.(6) [19]:

$$R_L = 1/1 + K_L C_0 \quad (6)$$

Where K_L (Lmg^{-1}) is the Langmuir constant described above and C_o (mg L^{-1}) is the initial amount of adsorbate. The R_L parameter is a more reliable indicator of adsorption. There are four probabilities for the R_L value: for favorable adsorption $0 < R_L < 1$, for unfavorable adsorption $R_L > 1$, for linear adsorption $R_L = 1$ and for irreversible adsorption $R_L = 0$.

The Freundlich isotherm was derived on the premise that adsorption takes place on heterogeneous surfaces and in multilayers. Eq (7) of the Freundlich model in the linear form [20]:

$$log\ q_e = log\ K_f + 1/n\ log\ C_e \quad (7)$$

The constant K_f (mg g^{-1}) is related to the adsorption capacity and. The value of n varies with the adsorbent's heterogeneity and a value of n >1 indicates a good adsorption process. The intercept and slope of the linear plot of $logq_e$ vs $logC_e$, respectively, define the values of K_f and n.

The Temkin isotherm was based on assuming a linear rather than logarithmic fall in the heat of sorption, as predicted by the Freundlich equation. Eq.(8) is how it's written [21]:

$$q_e = RT/b_T\ ln\ K_T + RT/b_T\ ln\ C_e \quad (8)$$

RT/b is the heat of adsorption, T the temperature (K), R the universal gas constant (J mol^{-1} K^{-1}), K_T is the equilibrium binding constant (Lmg^{-1}) corresponding to the maximum binding energy and b_T the variation of adsorption energy (J mol^{-1}).

3. Results and discussion

3.1. Characterization of SCBBPU

As shown in **Table 1**, it can be seen that SCBBPU has a low amount of moisture, volatiles, ash content and bulk density, which indicates that it is an excellent absorbent material. The high carbon yield is more favorable for the absorption process.

Because of the hysteresis loop between the adsorption and desorption branches, the SCBBPU Nitrogen adsorption-desorption isotherm are type I according to the IUPAC classification as shown in **Fig. 2**. The size of the pores was determined using N_2 desorption isotherms and the Barrett–Joyner–Halenda (BJH) method; the results suggest that the pores of SCBBPU are mostly in the 2–10 nm range and do not have macropores. Micropore filling is advantageous in low-pressure areas. A steep increase over 0.25 relative pressure in the SCBBPU adsorption isotherm indicated a wide range of micropore distribution. The multi-point Brunauer–Emmet–Teller (BET) method was used to calculate the total specific surface areas (SBET) of SCBBPU.

The crystalline structure of activated carbon was determined via XRD analysis. **Fig. 3.** Shows that the XRD pattern of SCBBPU sharp peaks observed in 2ɵ=26, 28, and 31, corresponds to the (002) planes of the graphitic structure. Therefore, the crystalline structure of SCBBPU is amorphous and graphitic.

The external surfaces of raw SCB show the particles have fibrous character. The surface has a compacted layer nature, with thin cellulose material layers resting one on top of each other, smooth and rough with irregular pores. The external surface of SCBBPU is different from SCB is appears a bubbly shape due to the prescience of polyurethane to enhance the adsorption of cationic dye **Figs. 4a and b.** Show SEM images of the SCB and SCBBPU, respectively.

The FTIR spectra of SCBBPU in the wavenumber range of 4000–400 cm^{-1} were shown in **Fig. 5.** The spectrum peak at 3419.84 cm^{-1} is attributed to –OH and –NH groups [22]. The band from 3200–3450 cm^{-1} has been assigned to the –NH absorption band of the urethane groups (–NHCOO–) as a result of modification SCB with polyurethane. The Strong peak at the band at 1640.37 cm^{-1} is C=C aromatic ring stretching vibrations. The peak observed at1400.24 cm^{-1} is attributed to C = C–H in-plane bending indicating several bands in cellulose and xylose. The adsorption at 1300–900 cm^{-1} with the peak at 1163.09–1000.95 cm^{-1} was tentatively assigned to the following phosphorous species and hydrogen-bonded P=O, O–C stretching vibrations in P–O–C of aromatics and P=OOH [11].

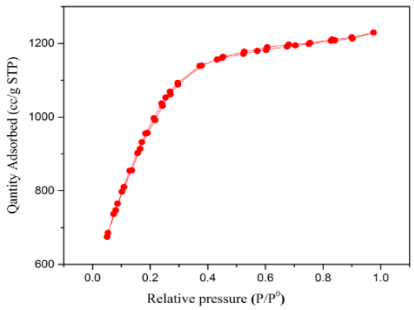

Fig. 2. Nitrogen adsorption-desorption isotherm

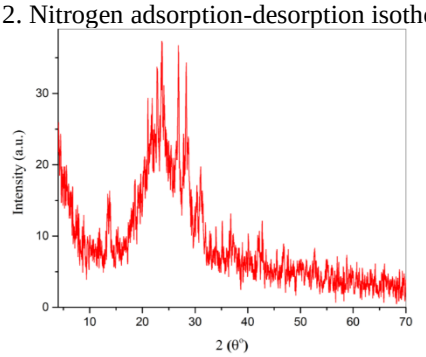

Fig. 3. XRD spectrum of SCBBPU

Table 1 Physical parameters of SCBBPU

Parameters	**SCBBPU**
Carbon yield (%)	55.3
Moisture content (%)	10
Volatile matter (%)	18
Ash content (%)	20
Bulk density (g/L)	0.018
pH_{PZC}	6.65
Total Pore Volume (cm^3/g)	2.47802
Average Pore Size (nm)	1.07792
BET Surface area (m^2/g)	3536.75

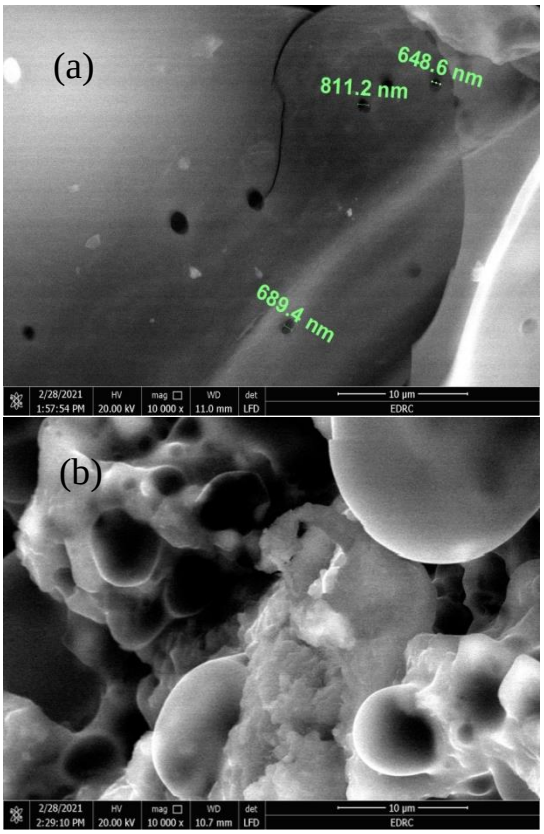

Fig. 4. SEM images of SCB (a) and SCBBPU (b) at magnification of 10 000×

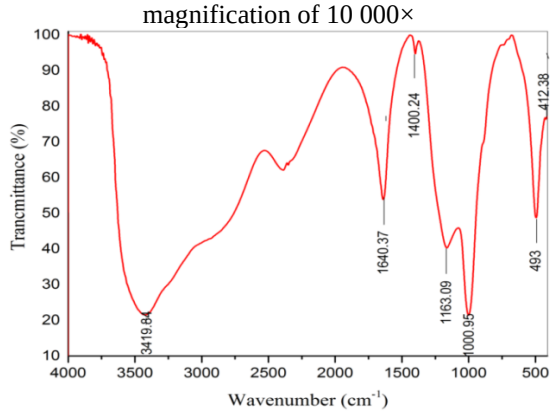

Fig. 5. FTIR spectra of SCBBPU

3.2. Effect of pH

The capacity and mechanism of adsorption are both influenced by the pH of the solution. Experiments occurred at Initial Concentration 9ppm, dosage 0.05g of SCBBPU and 25± 2 °C for 100 min. The pH of solutions had been adjusted between 3 - 9 by adding a few drops of aqueous 0.1M HCl and 0.1M NaOH. The pH of each suspension was measured using a pH meter. The percentage removal efficiency increased from 30.96% at pH 3.0 to 99.46% at pH 7.0, adsorption capacity increased from 0.3317 mg/g at pH 3 to 1.0656 mg/g at pH 7. Therefore, the optimum pH was recorded at pH 7 and the subsequent experiments were carried out at this pH. CV adsorption on activated carbon across a wide pH range is illustrated in. **Fig. 6**. As can be shown, the adsorption CV is smaller at pH 3, and then increases to higher values at pH 7[23, 24]. If the pH of the solution exceeds the pHPZC, the negative charge density on the surface of activated carbon increases, facilitating dye sorption [24]. In water, crystal violet forms both a cation (C+) and a reduced ion (CH+). Furthermore, in an acidic solution, the basic dye will become protonated, and the strength of the positive change will be greater on dye molecules with a lower pH, resulting in a decrease in their uptake. The surface of SCBBPU becomes negatively charged as the pH of the CV dye solution rises, facilitating the adsorption of the positively charged cationic dye through electrostatic attraction [25, 26].

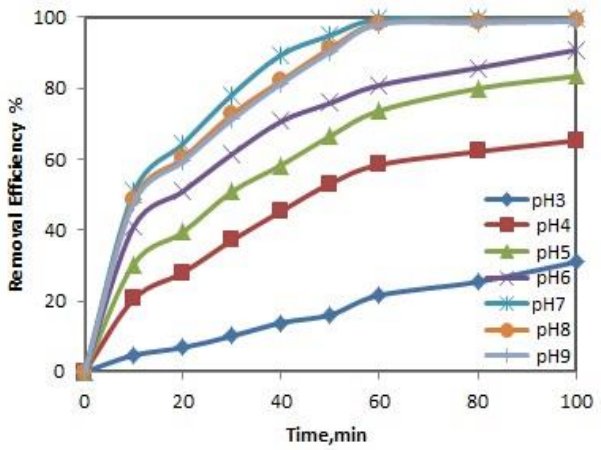

Fig. 6. Effect of pH under conditions: (initial CV concentration 9ppm, SCBBPU:0.05 g, stirring 200 rpm, time 100 min and Temp. 25 ± 2 °C)

3.3. Effect of Adsorbent Doses

The absorption of CV by SCBBPU was investigated using dosages (0.01-0.05)g at a dye concentration of 9ppm to determine the ideal absorption condition. **Fig. 7**. Because of the increased number of adsorption sites, the percentage removal efficiency of CV increases continuously as the SCBBPU dosage increases [27]. The percentage removal efficiency increases as the SCBBPU dosage increases from 0.01 to 0.05 g, from 55.88 percent at 0.01 g to 99.46 percent at 0.05 g. The removal efficiency is practically complete at 0.05 g, and it remains unchanged over this amount. Therefore, the optimum adsorbent dose was recorded at 0.05 and the subsequent experiments were carried out at this dose while adsorption capacity decreased from 2.9935mg/g at 0.01g to 1.0656mg/g at 0.05g.The maximum adsorption capacity q_e was observed at the lowest adsorbent dose [28].

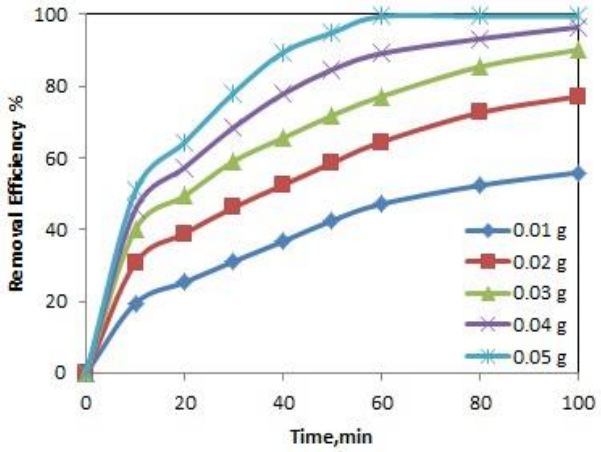

Fig. 7. Effect of Adsorbent Dosages SCBBPU under conditions: (initial CV concentration 9ppm, pH7, stirring 200 rpm, time 100 min and Temp. 25 ± 2 °C)

3.4. Effect of Initial dyes Concentration

The dye absorption mechanism is highly dependent on the dye concentration at the start. Several studies were carried out to determine the optimum dye concentration solution by adjusting the initial dye concentrations (3, 6, 9, 12, and 15) ppm to determine the ideal absorption condition for (0-100) min. **Fig. 8**. The highest amount of CV removed from the solution is 9 ppm. Therefore, the optimum initial dye concentration was recorded at 9ppm, and the subsequent experiments were carried out at this concentration. It has been discovered that as starting concentrations rise, the adsorption capacity rises from 0.3962 to 1.5579 mg/g while the percent dye removal decreases from 98.8 % to 88.76% when the initial concentration of CV increases from 3 to 15 ppm. After the optimum initial dye concentiration, specific sites become saturated and all active adsorption sites are occupied, preventing the adsorbent from adsorbing any more dye molecules [29, 30]. As a result, by diluting wastewaters with high dye concentrations, the purification yield can be boosted [31].

3.5. Effect of Temperature

Batch adsorption studies were conducted at various temperatures (25, 35, 45, and 55) °C, as indicated in **Fig. 9**. At 55°C, the percentage elimination effectiveness of CV increases from 99.46% at 25°C to 99.9%. The dye uptake for SCBBPU increased with increasing temperature (from 1.0656 to 1.0703mg/g), according to the results. The fact that absorption increased as the temperature increased refers to the systems being endothermic, suggesting that chemisorption occurred. The formation of hydrogen bonds between the adsorbate and the adsorbent is responsible for this. As a result, adsorption capacity should be dictated primarily by chemical interactions between functional groups on the adsorbent surface and the adsorbate and should increase as temperature increases. Because diffusion is an endothermic process, a faster rate of adsorption of the adsorbate into the pores of the adsorbent at higher temperatures may contribute to CV adsorption [32]. Finally, we get the best removal at the optimum conditions pH 7, initial dye concentration 9 ppm, adsorbent dose 0.05, contact time 100 min and temperature 55 °C, and maximum CV removal of 99.9% it is an excellent adsorbent when compared with the adsorption of crystal violet (CV) from aqueous solution by sugarcane bagasse (SCB), was investigated under conditions pH = 8.0, initial dye concentration = 200 mg L–1 and adsorbent dose = 2.0 g L–1, maximum CV removal of 93.21% was achieved under the optimized conditions [33].

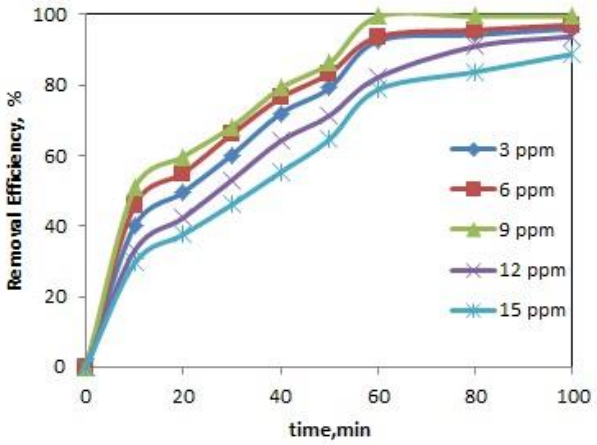

Fig. 8. Effect of the Initial CV Concentration under conditions: (pH 7, SCBBPU:0.05 g, stirring 200 rpm, time 100 min and Temp. 25 ± 2 °C)

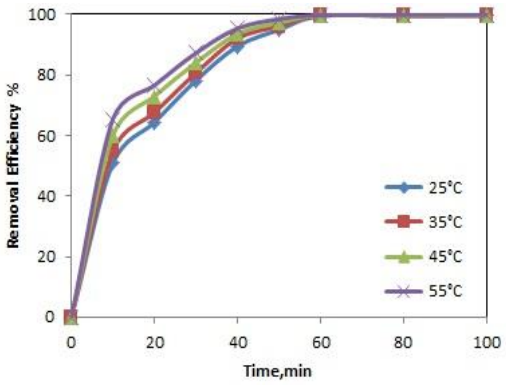

Fig. 9. Effect of Temperature under conditions: (initial CV concentration 15pp, pH 7, SCBBPU: 0.05g, stirring 200 rpm and time 100 min)

3.6. Adsorption kinetics

Adsorption kinetics is significant since it determines how efficient a process is and how long it takes to reach equilibrium. It also refers to the rate at which adsorbates are absorbed by activated carbon. Two kinetic models were explored and utilized to fit the experimental data from the adsorption of CV dye onto SCBBPU in order to determine the probable rate-controlling processes involved in the adsorption process. These models are the pseudo-first-order and pseudo-second-order kinetic models, the calculated parameters of all kinetic models are summarized in **Table 2. Fig. 10**. Show the correlation coefficients (R^2) value for the pseudo-first-order model. Besides, the experimental q_e values, $q_{e,\ exp}$ did not agree with the calculated values, $q_{e,\ cal}$ obtained from the linear plots. It means that the kinetics of CV adsorption on SCBBPU did not follow the pseudo-first-order kinetic model, and hence that the event displayed in **Fig. 11** was not a diffusion-controlled phenomenon. This method is more inclined to consider behavior across the entire adsorption range. The linear plot indicates that the experimental and estimated qe values are in good agreement. Furthermore, the pseudo-second-order kinetic model's related correlation coefficients (R^2) value indicates that the pseudo-second-order kinetic model may be used to describe the adsorption process of CV onto SCBBPU. Electrostatic interaction between the charged surface and charged dye molecules could produce dye adsorption, as well as the chemical characteristics of the activated carbon and dye molecules. It was suggested that chemisorption controlled the adsorption of CV onto SCBBPU [34].

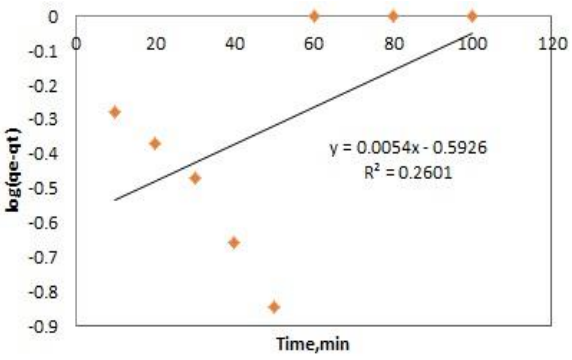

Fig. 10. Pseudo-first-order kinetics for adsorption of CV onto SCBBPU

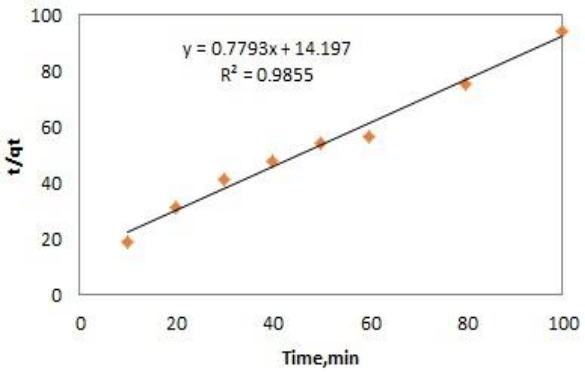

Fig. 11. Pseudo-second-order kinetics for adsorption of CV onto SCBBPU

Table 2 Kinetics parameters

Kinetics model	Parameters	CV dye
Pseudo-first order	q_e (mg g^{-1})	0.255
	k_1 (min^{-1})	0.0124
	R^2	0.2601
Pseudo-second order	$q_{e,exp}$ (mg g^{-1})	1.0656
	$q_{e,\ cal}$ (mg g^{-1})	1.283
	k_2 (g mg^{-1} min^{-1})	0.0427
	R^2	0.9855

3.7. Adsorption Isotherms

When the adsorption process reaches equilibrium, the adsorption isotherm shows how the adsorption molecules are distributed across the liquid and solid phases. The fitting of isotherm data to various isotherm models is a crucial step in determining the most appropriate model for design purposes [35].The isotherm data were fitted to the Langmuir, Freundlich, and Temkin isotherms models at several temperatures (298 - 328)K are summarized in **Table 3 and Figs. 12, 13, 14**. The Langmuir adsorption isotherm has been successfully applied to the adsorption of numerous contaminants and is the most extensively utilized sorption isotherm for the sorption of a solute from a liquid solution [26]. The Langmuir isotherm model predicts the development of a monolayer of dye on the adsorbent's outer surface. The Langmuir equation assumes that intermolecular interactions decrease fast with distance and that monolayer adsorption occurs on the adsorbent's outer surface, with homogeneous adsorption sites. **Table 3** summarizes the highest adsorption capacity of CV determined by Langmuir isotherm studies. As a result, the adsorption process matched the Langmuir isotherm model, indicating that a monolayer adsorption mechanism took place on the outer surface of the adsorbent. The Freundlich isotherm, on the other hand, proposes that adsorption takes place on heterogeneous surfaces at sites with varied adsorption energies and non-identical adsorption sites that aren't always available [36, 37].Mathematically it is characterized by the heterogeneity factor '1/n'. The value of 1/n is related to the adsorption intensity it is well-known that the closer the n value to zero, the more heterogeneous the

system becomes [38]. The correlation coefficients (R^2) for four different temperatures are summarized in **Table 3** show (R^2 < 0.95) the value of correlation coefficients of Freundlich isotherm of CV low when compare with Langmuir isotherm so This indicates that the Freundlich model is not appropriate for modelling CV onto SCBBPU adsorption in this investigation. To analyze the sorbent's adsorption potentials for sorbate, the Temkin isotherm plot [39] was also used. Because of sorbate and sorbent interactions, the heat of sorption of the molecules in the layer falls linearly with coverage. The results of this study show that the adsorption process is engaged in chemical sorption. The correlation coefficients (R^2) calculated for CV fitting with the Langmuir equation is higher than those calculated using the Freundlich and Temkin equations. Because the experimental data reaching asaturation plateau at high C_e, Langmuir better describes the experimental system of CV adsorption. Freundlich and Temkin's models do not accommodate this saturation tendency.

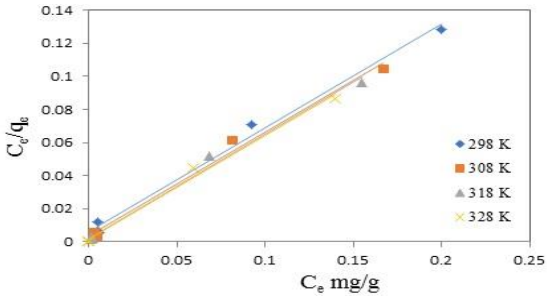

Fig. 12. Langmuir isotherm for adsorption of CV onto SCBBPU

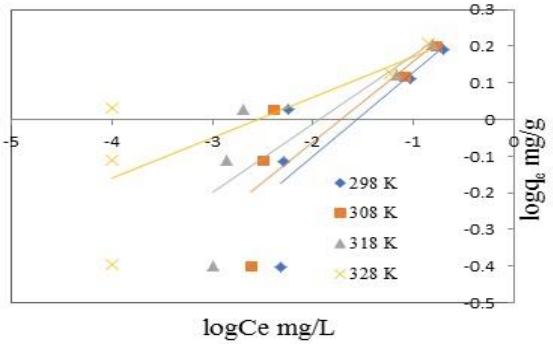

Fig. 13. Freundlich isotherm for adsorption of CV onto SCBBPU

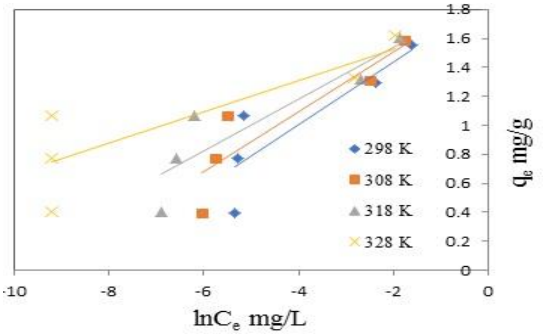

Fig. 14. Temkin isotherm for adsorption of CV onto SCBBPU

Table 3 Adsorption isotherm parameters

Adsorption Isotherm model	Parameters	Temperature (K)			
		298	308	318	328
Langmuir	R^2	0.99	0.99	0.99	0.99
	q_0 (mg g^{-1})	1.59	1.59	1.59	1.59
	K_L(L/g)	0.10	0.16	0.26	0.48
	R_L	0.84	0.77	0.68	0.54
Freundlich	R^2	0.59	0.65	0.67	0.57
	K_F (mg g^{-1})	2.27	2.39	2.31	1.91
	n (mg g^{-1})	4.37	4.55	5.33	9.02
Temkin	R^2	0.74	0.801	0.81	0.72
	K_T	0.02	0.02	0.28	0.04
	b_T (kJ mol^{-1})	11.4	12.3	14.8	25.2

3.8. Evaluation of thermodynamic parameters

Thermodynamic studies are required to determine the viability of adsorption procedures carried out at various temperatures, as well as to assess the nature of the reaction.

$$\Delta G^0 = -RT \ln K_d \quad (15)$$

$$\ln K_d = \Delta S^0/R - \Delta H^0/R \quad (16)$$

$$\Delta G^0 = \Delta H^0 = T\Delta S \quad (17)$$

Enthalpy change and other thermodynamic parameters ΔH° is the change in enthalpy (kJ/mol), ΔG° is the change in Gibbs energy (kJ/mol), and ΔS° is the change in entropy (J/mol. K) can be calculated using equilibrium constants that fluctuate with temperature. **Table 3** shows the values of standard Gibbs free energy change for the adsorption process based on K_d values obtained from the Langmuir model at various temperatures [40]. The absorption reaction's Gibbs free energy change is provided by the equation below (18).

$$\Delta G^0 = -RT\ln K_d = -RTK \quad (18)$$

T is the absolute temperature (K), and R is the universal gas constant (8.314 $Jmol^{-1}$ K^{-1}). The equilibrium constants can be stated in terms of enthalpy change of temperature adsorption as shown in **Table 3**..

$$d\ln K_d/dT = \Delta H^0/RT^2 \quad (19)$$

The sign of ΔH determines the effect of temperature on the equilibrium constant K_d, according to Eq. (19). When ΔH is positive, the adsorption is endothermic, and T is increased, K_d increases. When ΔH is negative, indicating exothermic adsorption, a rise in T induces a reduction in K_d. The free energy change and the equilibrium constant can be described as follows as a function of temperature.

$$\Delta G^0 = \Delta H^0 - T\Delta S^0 \quad (20)$$

$$\ln K_d = \Delta S^0/R - \Delta H^0/RT \quad (21)$$

Based on the above equations, the parameters of thermochemical reaction ΔS° and ΔH° can be determined from the intercept and slope of the linear plot of van't Hoff between $\ln k_d$ vs. 1/T, respectively. As a result, based on entropy (ΔS°) and enthalpy (ΔH°), the values of ΔG° at various temperatures may be calculated to characterize the most appropriate adsorption behaviour for the current experimental data. **Fig.15**. Thermodynamic

considerations revealed that ΔG° values are the most important element in detecting adsorption properties. The slope of ΔG° as a function of temperature suggested that temperature aids the adsorption process [41]. The negative values of Gibbs free energy change (ΔG°) confirmed that the adsorption of CV onto SCBBPU was spontaneous. The endothermic nature of CV adsorption on SCBBPU was shown by the positive H° readings. Increased adsorption unpredictability at the solid-liquid interface was likely represented by the growing positive value of S°. Values of thermodynamic parameters for the adsorption of CV onto SCBBPU are summarized in **Table 4**

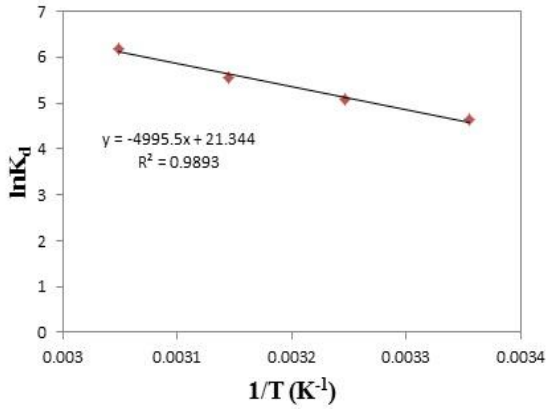

Fig. 15. Van't Hoff plot for adsorption of CV onto SCBBPU

Table 4 Values of Thermodynamic parameters

Dye	T (K)	lnKd	ΔH° (kJ/ mol)	ΔS° (J/ mol K)	ΔG° (kJ/ mol)
CV	298	4.63	41.5	177.4	-11.47
	308	5.078			-13.003
	318	5.564			-14.7
	328	6.179			-16.85

Conclusion

The adsorption of CV from aqueous solution was found to be highly influenced by pH, SCBBPU doses, contact time, temperature, and CV initial concentration. The adsorption of SCBBPU was well explained by the chemisorption model of pseudo-second-order kinetics, according to the kinetic investigations. Three adsorption isotherm models, the Langmuir, Freundlich, and Temkin isotherm models, were used to assess the experimental results. Furthermore, it was demonstrated that the experimental data obtained for CV adsorption onto SCBBPU match to the Langmuir isotherm model. The thermodynamic parameter ΔG° was studied, and negative values demonstrated that CV adsorption onto SCBBPU was spontaneous, but the incline of ΔG° as a function of temperature indicated that warmth aids the adsorption process. The positive ΔH° and ΔS° data indicated that the adsorption of CV on SCBBPU was an endothermic process and that the process was becoming more random. As a result, the yield of SCBBPU shows that it is an excellent, effective, and low-cost adsorbent for dye removal from wastewater.

Conflicts of interest

The authors declare that they have no conflicts of interest.

Formatting of funding sources

No funding sources

Acknowledgments

Both authors would like to thank Menoufia University to support present research and the required devices. Special thanks devoted to the staff of Central Laboratory for Environmental Quality Monitoring for their cooperation during measurements for providing necessary facilities to accomplish the work.

References

[1] Madrakian, T., Afkhami, A., Mahmood-Kashani, H., & Ahmadi, M. (2013). Adsorption of some cationic and anionic dyes on magnetite nanoparticles-modified activated carbon from aqueous solutions: equilibrium and kinetics study. Journal of the Iranian Chemical Society, 10(3), 481-489.

[2] Hassaan, M. A., El Nemr, A., & Hassaan, A. (2017). Health and environmental impacts of dyes: mini review. American Journal of Environmental Science and Engineering, 1(3), 64-67.

[3] Haldorai, Y., & Shim, J. J. (2014). An efficient removal of methyl orange dye from aqueous solution by adsorption onto chitosan/MgO composite: A novel reusable adsorbent. Applied surface science, 292, 447-453.

[4] Saeed, A., Sharif, M., & Iqbal, M. (2010). Application potential of grapefruit peel as dye sorbent: kinetics, equilibrium and mechanism of crystal violet adsorption. Journal of hazardous materials, 179(1-3), 564-572.

[5] Ahmed, M., Mashkoor, F., & Nasar, A. (2020). Development, characterization, and utilization of magnetized orange peel waste as a novel adsorbent for the confiscation of crystal violet dye from aqueous solution. Groundwater for Sustainable Development, 10, 100322.

[6] Lin, Y. C., Ho, S. H., Zhou, Y., & Ren, N. Q.(2018).Highly efficient adsorption of dyes by biochar derived from pigments-extracted macroalgae pyrolyzed at different temperature. Bioresource technology, 259, 104-110.

[7] Tehrani-Bagha, A. R., Mahmoodi, N. M., & Menger, F. M. (2010). Degradation of a persistent organic dye from colored textile wastewater by ozonation. Desalination, 260(1-3), 34-38.

[8] Qianqian, Z., Tang, B., & Guoxin, H. (2011). High photoactive and visible-light responsive graphene/titanate nanotubes photocatalysts:

Preparation and characterization. Journal of hazardous materials, 198, 78-86.
[9] Alventosa-deLara, E., Barredo-Damas, S., Alcaina-Miranda, M. I., & Iborra-Clar, M. I. (2012). Ultrafiltration technology with a ceramic membrane for reactive dye removal: optimization of membrane performance. Journal of hazardous materials, 209, 492-500.
[10] Ghaedi, M., Hajati, S., Barazesh, B., Karimi, F., & Ghezelbash, G. (2013). Saccharomyces cerevisiae for the biosorption of basic dyes from binary component systems and the high order derivative spectrophotometric method for simultaneous analysis of Brilliant green and Methylene blue. Journal of Industrial and Engineering Chemistry, 19(1), 227-233.
[11] Han, Q., Wang, J., Goodman, B. A., Xie, J., & Liu, Z. (2020). High adsorption of methylene blue by activated carbon prepared from phosphoric acid treated eucalyptus residue. Powder Technology, 366, 239-248.
[12] Azimi, S. C., Shirini, F., & Pendashteh, A. R. ٢٠٢١)). Advanced oxidation process as a green technology for dyes removal from wastewater: A review. Iranian Journal of Chemistry and Chemical Engineering (IJCCE), 40(5), 1467-1489.
[13] Zou, H., Chu, L., & Wang, Y.(2019). Azo dye wastewater treatment in a novel process of biofilm coupled with electrolysis. Archives of Environmental Protection, 45(3).
[14] Subbaiah, M. V., & Kim, D. S. (2016). Adsorption of methyl orange from aqueous solution by aminated pumpkin seed powder: Kinetics, isotherms, and thermodynamic studies. Ecotoxicology and environmental safety, 128, 109-117.
[15] Sajab, M. S., Chia, C. H., Zakaria, S., & Khiew, P. S. (2013). Cationic and anionic modifications of oil palm empty fruit bunch fibers for the removal of dyes from aqueous solutions. Bioresource Technology, 128, 571-577.
[16] Lagergren, S. (1898). Zur theorie der sogenannten adsorption geloster stoffe.
[17] Ho, Y. S., & McKay, G. (1999). Pseudo-second order model for sorption processes. Process biochemistry, 34(5), 451-465.
[18] Langmuir, I. (1918). The adsorption of gases on plane surfaces of glass, mica and platinum. Journal of the American Chemical society, 40(9), 1361-1403.
[19] Hall, K. R., Eagleton, L. C., Acrivos, A., & Vermeulen, T. (1966). Pore-and solid-diffusion kinetics in fixed-bed adsorption under constant-pattern conditions. Industrial & Engineering Chemistry Fundamentals, 5(2), 212-223.
[20] Freundlich, H. M. F. (1906). Over the adsorption in solution. J. Phys. Chem, 57(385471), 1100-1107.
[21] Rajappa, A., Ramesh, K., Nandhakumar, V., & Ramesh, H. E. M. A. (2014). Equilibrium and isotherm studies of Congo red adsorption onto commercial activated carbon. Int. J. Curr. Res. Chem. Pharm. Sci, 1, 43-48.
[22] Song, X., Zhang, Y., & Chang, C. (2012). Novel method for preparing activated carbons with high specific surface area from rice husk. Industrial & engineering chemistry research, 51(46), 15075-15081.
[23] Sakin Omer, O., Hussein, M. A., Hussein, B. H. M., & Mgaidi, A. (2018). Adsorption thermodynamics of cationic dyes (methylene blue and crystal violet) to a natural clay mineral from aqueous solution between 293.15 and 323.15 K. Arabian Journal of Chemistry, 11(5), 615–623.
[24] Khan, M. M. R., Rahman, M. W., Ong, H. R., Ismail, A. B., & Cheng, C. K. (2015). Tea dust as a potential low-cost adsorbent for the removal of crystal violet from aqueous solution. Desalination and Water Treatment, 57(31), 14728–14738.
[25] Yagub, M. T., Sen, T. K., Afroze, S., & Ang, H. M. (2014). Dye and its removal from aqueous solution by adsorption: A review. Advances in Colloid and Interface Science, 209, 172–184.
[26] Salleh, M. A. M., Mahmoud, D. K., Karim, W. A. W. A., & Idris, A. (2011). Cationic and anionic dye adsorption by agricultural solid wastes: A comprehensive review. Desalination, 280(1-3), 1–13.
[27] Yagub, M. T., Sen, T. K., & Ang, H. M. (2012). Equilibrium, kinetics, and thermodynamics of methylene blue adsorption by pine tree leaves. Water, Air, & Soil Pollution, 223(8), 5267-5282.
[28] Basu, S., Ghosh, G., & Saha, S. (2018). Adsorption characteristics of phosphoric acid induced activation of bio-carbon: Equilibrium, kinetics, thermodynamics and batch adsorber design. Process Safety and Environmental Protection, 117, 125-142.
[29] Saeed, A., Sharif, M., & Iqbal, M. (2010). Application potential of grapefruit peel as dye sorbent: kinetics, equilibrium and mechanism of crystal violet adsorption. Journal of hazardous materials, 179(1-3), 564-572.
[30] Gebreslassie, Y. T.(2020). Equilibrium, kinetics, and thermodynamic studies of malachite green adsorption onto Fig (Ficus cartia) leaves. Journal of analytical methods in chemistry, 2020.
[31] Uzunoğlu, D., & Özer, A. (2016). Adsorption of Acid Blue 121 dye on fish (Dicentrarchus labrax) scales, the extracted from fish scales and commercial hydroxyapatite: equilibrium, kinetic, thermodynamic, and characterization studies. Desalination and Water Treatment, 57(30), 14109-14131.
[32] Sarabadan, M., Bashiri, H., & Mousavi, S. M. (2019). Removal of crystal violet dye by an efficient and low cost adsorbent: Modeling, kinetic, equilibrium and thermodynamic studies. Korean Journal of Chemical Engineering, 36(10), 1575-1586.
[33] Chakraborty, S., Chowdhury, S., & Saha, P. D. (2012). Adsorption of crystal violet from aqueous solution onto sugarcane bagasse: central composite design for optimization of process variables. Journal of Water Reuse and Desalination, 2(1), 55-65.
[34] Wang, Y., Chen, T., Zhang, X., & Mwamulima, T. (2021). Removal Study of Crystal Violet and Methylene Blue From Aqueous Solution by Activated Carbon Embedded Zero-Valent Iron: Effect of Reduction Methods. Frontiers in Environmental Science, 631.
[35] Yagub, M. T., Sen, T. K., Afroze, S., & Ang, H. M. (2014). Dye and its removal from aqueous

solution by adsorption: a review. Advances in colloid and interface science, 209, 172-184.
[36] Alharby, N. F., Almutairi, R. S., & Mohamed, N. A. (2021). Adsorption Behavior of Methylene Blue Dye by Novel Crosslinked O-CM-Chitosan Hydrogel in Aqueous Solution: Kinetics, Isotherm and Thermodynamics. Polymers, 13(21), 3659.
[37] Coskun, R., Savci, S., & Delibas, A. (2018). Adsorption properties of activated almond shells for methylene blue (MB). Environmental Research and Technology, 1(2), 31-38.
[38] Sulyman, M., Namieśnik, J., & Gierak, A. (2016). Adsorptive removal of aqueous phase crystal violet dye by low-cost activated carbon obtained from Date palm (L.) dead leaflets. Inżynieria i Ochrona Środowiska, 19.
[39] Ghasemian, E., & Palizban, Z. (2016). Comparisons of azo dye adsorptions onto activated carbon and silicon carbide nanoparticles loaded on activated carbon. International journal of environmental science and technology, 13(2), 501-512.
[40] Chen, S., Zhang, J., Zhang, C., Yue, Q., Li, Y., & Li, C. (2010). Equilibrium and kinetic studies of methyl orange and methyl violet adsorption on activated carbon derived from Phragmites australis. Desalination, 252(1-3), 149-156.
[41] Senthilkumaar, S., Kalaamani, P., & Subburaam, C. V. (2006). Liquid phase adsorption of crystal violet onto activated carbons derived from male flowers of coconut tree. Journal of hazardous materials, 136(3), 800-808.